Journal of Polymer Research (2022) 29: 194
https://doi.org/10.1007/s10965-022-03054-x

ORIGINAL PAPER

Preparation and application of poly(α-L-lysine)-based interpenetrating network hydrogel via synchronous free-radical polymerization and amine-anhydride reaction in water

Chunwang Hu[1] · Hongliang Wei[1] · Bingyan Hua[1] · Yaqi Zhang[1] · Gang Wang[1] · Yanmin Shen[1] · Yongsheng Niu[1,2]

Received: 2 January 2022 / Accepted: 25 April 2022 / Published online: 2 May 2022

Abstract

Drug- controlled delivery can effectively avoid excessive drug use and improve the utilization rate of drugs and reduce the harm of drugs to the body. Herein, a novel poly(α-L-lysine)-based interpenetrating network (IPN) hydrogel with thermo/pH sensitivity was fabricated by synchronous free-radical polymerization and amine-anhydride click reaction in one pot. The hydrogels were characterized by FTIR, X-ray diffraction (XRD), and scanning electron microscopy (SEM). The IPN hydrogels well integrated thermo-sensitivity and pH-sensitivity of two single-network hydrogels. The experimental results showed that the IPN hydrogel exhibited different swelling properties at different pH and temperatures. Finally, the anticancer drug 5-fluorouracil (5-Fu) was chosen as a model drug to investigate the controlled release behavior of the hydrogel. The study showed that the release behavior of 5-Fu from the IPN hydrogel depended on temperature and pH changes, which followed the Korsmeyer-Peppas kinetic model. The IPN hydrogel is expected to be a candidate material for drug sustained-release carriers.

Keywords Interpenetrating network · Poly(α-L-lysine) · Click reaction · Hydrogel · Sensitivity

Introduction

Hydrogel is a kind of three-dimensional cross-linked polymeric network which can absorb a large amount of water in an aqueous solution to cause a rapid increase in volume but is insoluble in water [1]. Due to the excellent water absorption, flexibility, and biocompatibility of hydrogel, the hydrogel has become a significant research area in drug delivery systems [2], which can prolong the retention time of the drug and slow down the release rate of the drug. However, a traditional hydrogel cannot control and target drugs to desired parts of the body. Different drugs need to meet different release behavior to achieve the best therapeutic effect, so the drug-carrier should be able to vary its properties according to the environment. Under such a background, a hydrogel that can identify and react to the changes in normal physiological parameters has attracted extensive attention [3]. The smart hydrogel can respond to changes in external environmental stimuli such as pH, temperature, salt, electric, and magnetic fields [4]. These stimuli can affect the swelling degree, degradation rate and drug release rate of the hydrogel. Among them, the adjustment of pH and temperature is the easiest to achieve in the experiment, which has a significant impact on the properties of the hydrogel. Additionally, the change of pH and temperature is also ubiquity in nature and organisms.

pH-sensitive hydrogel contains protonated groups, such as amine and carboxyl groups, which can gain or lose protons depending on the change of pH, thus causing the volume change of hydrogels [5]. When pH-sensitive hydrogels are used as drug release carriers, the change of environmental pH causes their volume to shrink or swell, thereby controlling the drug release rate and optimizing the therapeutic effect [6]. pH-sensitive hydrogels also have high application value in biosensors. For example, in the application of wearable and portable biosensors, pH-sensitive hydrogels can predict the physical condition of the human body via making

✉ Hongliang Wei
weihl68@126.com

✉ Yongsheng Niu
nys2205@163.com

[1] School of Chemistry and Chemical Engineering, Henan University of Technology, 450001 Zhengzhou, PR China

[2] College of Chemistry and Environmental Engineering, Anyang Institute of Technology, Anyang, PR China

corresponding response behavior according to the change of pH value of human sweat. [7].

Different from pH- sensitive hydrogels, thermo-sensitive smart hydrogels have a volume phase transition temperature (VPTT), where a significant shrinkage or expansion of volume occurs. Poly(N-vinyl caprolactam) [8], poly(oligo(ethylene glycol) methacrylate) [9], and poly(N-isopropyl acrylamide) (PNIPAm) have been widely applied in the preparation of smart hydrogels as temperature-sensitive materials. Among them, PNIPAm has been widely studied because its low critical solution temperature (LCST) is close to the temperature of the human body. When the ambient temperature is lower than the LCST, the PNIPAm hydrogel quickly absorbs water and swells. On the contrary, when the temperature is higher than the LCST, the PNIPAm hydrogel shrinks and removes water [10]. However, the traditional PNIPAm hydrogel usually uses small molecule N, N-methylene bisacrylamide as the chemical crosslinking agent, which leads to the brittleness of the hydrogel and limits its further applications [11].

Additionally, crosslinking methods have a significant influence on the properties of hydrogels. According to crosslinking mechanism, the preparation methods of hydrogels can be generally divided into physical crosslinking and chemical crosslinking [12]. Physically cross-linked hydrogels are networks obtained by non-covalent bonds, such as van der Waals forces, hydrogen bonds, or electrostatic interaction. The formation of such hydrogels is reversible because the molecular chains are physically cross-linked. When external conditions such as temperature change, the physical crosslinking points will be destroyed [13]. Therefore, physical gels are also called reversible gels. Chemical crosslinking hydrogels refer to networks formed by covalent bonds, which are relatively stable. Standard chemical crosslinking methods include free-radical polymerization, Michael addition reaction, Schiff base reaction, and click reaction [14]. Among them, click reaction provides a wide range of bond stability for network structure [15] and is an elegant means for adjusting the physicochemical properties of hydrogels in a controlled manner [16]. Click reaction is a term for describing a class of reactions with the characteristics of modularization, rapidity, high efficiency, and easy manipulation, including nucleophilic ring opening reaction, carbon-carbon multibond addition reaction, etc. Nowadays, the scope of coverage of click reactions is expanding; for instance, amine-aldehyde reaction, amine-epoxy reaction, thiol-epoxy reaction, thiol-isocyanate reaction, thiol-alkyne reaction can also be grouped under click reaction. In our lab, we observed that gelation could occur rapidly in an aqueous solution through an efficient and mild amine-anhydride reaction without isolating air, which conforms to the characteristics of click reaction. Therefore, we studied the application of amine-anhydride reaction in the preparation of hydrogels.

Generally, raw materials for preparing a hydrogel can be divided into natural raw materials and synthetic raw materials [17]. The properties of hydrogels prepared from synthetic polymer materials can be adjusted more flexibly [18]. Acrylic acid, acrylamide, N-isopropyl acrylamide, and other synthetic raw materials have been widely used to synthesize hydrogels. Hydrogels prepared from natural raw materials such as proteins and polysaccharides have the characteristics of non-toxicity, good biodegradability, and biocompatibility. Still, their poor mechanical strength limits their wide range of applications [19]. Poly-L-Lysine (PLL) is a cationic biopolymer containing the monomeric unit L-lysine. There are two types of PLL, α-PLL and ε-PLL. Both possess naturally inherent properties, e.g., environmental friendliness and non-antigenicity [20, 21]. Of those, α-PLL is the most well studied [22]. Due to their intrinsic merits, PLL-based hydrogels have been applied widely in various fields [23].

To improve the performance of hydrogels, scientists have proposed a series of optimization schemes [24]. For example, grafting polymers containing different side chains, forming comb-shaped grafted hydrogels, fabricating interpenetrating network structures, and combining composite nanomaterials. The interpenetrating network provides a new and stable structure for the hydrogel. Through the synergy of the two networks, its performance is significantly better than the corresponding single-network hydrogel, which displays significant advantages in applications. Therefore, forming an interpenetrating network structure is the most commonly used method to increase the mechanical properties, thermal stability, and chemical stability of hydrogels [25]. According to the synthesis method, IPN hydrogels are subdivided into two categories: stepwise IPN hydrogels and synchronous IPN hydrogels [26]. The stepwise IPN refers to forming a network first, and then putting the network to another monomer or prepolymer solution to create a second network through a crosslinking reaction, which is usually time-consuming and inconvenient. For example, Saruchi et al. synthesized an IPN hydrogel using natural polysaccharide gum tragacanth, acrylamide, and methacrylic acid by stepwise method, which was used for sustained release of soil fertilizer [27]. Synchronous IPN is to put all the raw materials used for forming the network in a container at the same time and fabricating different networks through their independent reaction processes, which is simple and especially adapted for preparing injectable hydrogels.

In this study, we proposed that an IPN hydrogel with thermo and pH sensitivity could be prepared via synchronous free-radical polymerization and amine-anhydride reaction in one pot. One hydrogel network with pH sensitivity was formed by an amine-anhydride reaction in water between the binary copolymer and natural material poly(α-L-lysine) (PLL). The other network with thermo-sensitivity was fabricated via free-radical polymerization of

N-isopropyl acrylamide and N, N-methylene bisacrylamide. The hydrogel exhibited dual temperature and pH sensitivity by forming an interpenetrating network structure. The controlled release behavior and the drug release mechanism of hydrogel were analyzed by choosing 5-Fu as a model drug. The preparation method of the IPN hydrogel is simple, and the reaction conditions are mild. 5-Fu is an effective chemotherapeutic anticancer drug but with some application limitations due to its low bioavailability and cytotoxic nature [28]. Therefore, developing a controlled targeted 5-Fu-carrier is necessary to improve its therapy and reduce its cytotoxicity [29]. To the best of our knowledge, there are many reports on amine-anhydride reaction in organic solvents, but the research on amine-anhydride click reaction in water for forming poly(α-L-lysine)-based IPN hydrogels is unexplored so far. Therefore, the study is of significance to the preparation of IPN hydrogel.

Materials and methods

Materials

N, N-dimethyl acrylamide (DMA), Poly(α-L-lysine) (PLL), N-isopropyl acrylamide (NIPAm), and N, N-methylene bisacrylamide (MBA) were obtained from Saen Chemical Technology (Shanghai) Co., Ltd, China. Maleic anhydride (MAH) was purchased from Shanghai Aladdin Biochemical Technology Co., Ltd, China. 2,2'-Azo-diisobutyronitrile (AIBN) was supplied by Tianjin Kemiou Chemical Reagent Co., Ltd, China. Potassium persulfate was purchased from Luoyang Haohua Chemical Reagent Co., Ltd, China. Ascorbic acid (Vc) was provided by Beijing Innochem Technology Co., Ltd, China. Triethylamine (Et_3N) was bought from Tianjin Tianli Chemical Reagent Co., Ltd, China. AIBN, potassium persulfate, and triethylamine were purified according to ordinary methods. Other reagents were analytically pure and had not been treated before use. Initiator solutions (0.15 mol/L) of potassium persulfate and ascorbic acid were prepared in advance and used for the related polymerization reaction.

Fabrication of hydrogel

Synthesis of the copolymer of MAH and DMA

Herein, a binary copolymer containing anhydride groups was synthesized by free-radical polymerization of MAH, and DMA using AIBN as an initiator. The molar ratio of MAH and DMA was set as 1: 50, the total concentration of the monomers was set as 1.0 mol/L, and the obtained binary copolymer was denoted as "PMD". Typically, the synthesis process of PMD is as follows: MAH (0.1154 g, 1.176 mmol), DMA (5.831 g, 58.824 mmol) and AIBN (0.0493 g, 0.300 mmol) were added to a round-bottom flask containing 60 mL 1, 4-dioxane and stirred with a magnetic mixer until completely dissolved. Then, the reaction system deoxygenated via vacuum-pumping and argon-filling cycles. The oil bath temperature was controlled at 75 °C, and the system was maintained under an argon atmosphere during the reaction period. After eight hours, the reaction solution was concentrated by a rotary evaporator and then dropped into 400 mL petroleum ether with constant stirring to obtain a white precipitate. The obtained white precipitate was washed with petroleum ether three times (50 mL each time), and then dried to constant weight under vacuum at 70 °C. The product yield was 97%.

Preparation of single network hydrogels based on the amine-anhydride reaction

Firstly, a certain amount of binary copolymer was weighed in a 10 mL small test tube, and 1.5 mL deionized water was added to dissolve the binary copolymer to obtain an aqueous solution. After an appropriate amount of poly(α-L-lysine) was dissolved in 0.5 mL deionized water, quantitative triethylamine was added to adjust the pH of the solution to alkalinity. Their raw material composition was presented in Table S1. Then the poly(α-L-lysine) solution was poured into a small test tube containing a binary copolymer and mixed evenly. Finally, the solution was put into a water bath of 50 °C and reacted for 15 min to form a gel. After gelation, it was kept at 50 °C for 6 h. The single-network hydrogels formed from amine-anhydride were named CN_n, where n was the molar ratio of amine groups to anhydride groups (Fig. 1A).

Preparation of single network hydrogel based on free-radical polymerization

NIPAm and MBA were charged into a 10 mL test tube, and then dissolved in 2.0 mL deionized water. Afterward, an appropriate amount of KPS and Vc solution was added into the tube and mixed evenly. Their raw material composition was presented in Table S2. The reaction was carried out for 40 min at room temperature to form a gel. The digital photos of hydrogels during preparation are shown in Fig. S1. The hydrogels formed from the free-radical polymerization of NIPAm and MBA were named PN_n, where n was the mole ratio of NIPAm and MBA (Fig. 1B).

Preparation of IPN hydrogel

The binary copolymer PMD and NIPAm were weighed and put in a 10 mL test tube, and then 1.5 mL deionized water was added to dissolve them. Poly(α-L-lysine) and MBA were

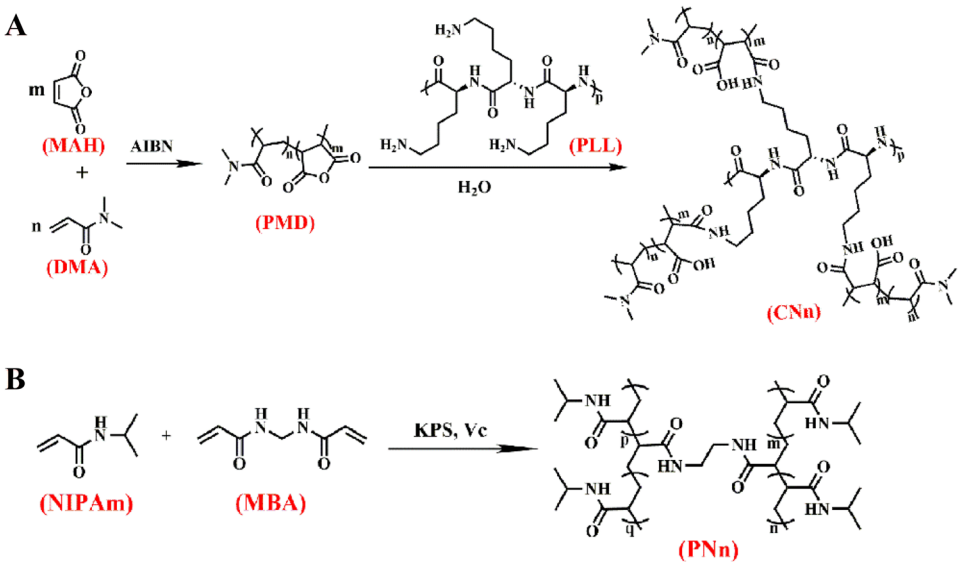

Fig. 1 Synthesis mechanism of CN_n (**A**) and PN_n (**B**) hydrogels

weighed and put in a small beaker, and then 0.5 mL deionized water was used to dissolve them to obtain a solution. The solution was poured into the test tube, then KPS and Vc solution and triethylamine were added and mixed well. The raw material composition of IPN-Gel was presented in Table S3. The tube was put into a water bath of 50 °C, and the gelation was observed within 10 min. After gelation, it was kept at 50 °C for 6 h. The IPN hydrogels were denoted as $DN_{n\text{-}m}$, where n is the molar ratio of the amine group to the anhydride group, and m is the mole ratio of NIPAm to MBA (Fig. 2).

Preparation of 5-Fu-loaded hydrogel

The *In-situ* drug loading method was used to prepare drug-loaded hydrogels. In brief, similar to the above preparation method of hydrogel, 5-Fu was dissolved in initial deionized water (5-Fu: H_2O = 10 mg: 1 g) to obtain a 5-Fu aqueous solution. The raw material for preparing hydrogels was dissolved in a 5-Fu aqueous solution, and the hydrogels were prepared through the above steps. The prepared hydrogels were dried at 50 °C under atmospheric pressure until constant weight.

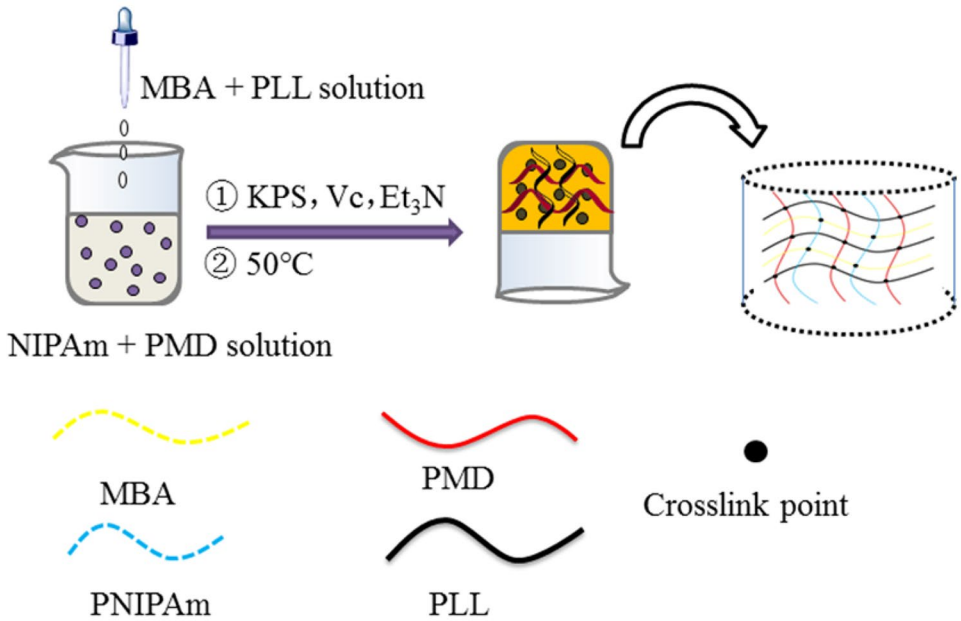

Fig. 2 The schematic diagram of the preparation process of IPN hydrogel

Characterization

FT-IR spectra of samples were obtained at room temperature utilizing an infrared spectrometer (PerkinElmer UATR Two, UK). The scanning range is between 4000 – 400 cm^{-1}. The hydrogel was soaked in deionized water at room temperature until its swelling reached equilibrium, and then frozen in the refrigerator for 24 h, and freeze-dried in a freeze-dryer. The morphology of single network hydrogels and interpenetrating network hydrogels was observed by scanning electron microscopy (JEOL JSM-6490 A, Tokyo, Japan). The aggregated structure of the hydrogels was determined by Rigaku Miniflex-600 X-ray diffractometer (Rigaku, Japan) in the Cu-K α radiation range of 5–90° with current and voltage of 100 mA and 40 kV, respectively.

Gel mass fraction

Gel mass fraction (GMF) was usually utilized to evaluate the degree of crosslinking of hydrogels. Typically, dry hydrogel samples (m_1) were soaked in deionized water at room temperature, and the water was changed every six hours to remove free molecules. After two days, the samples were taken out and dried to constant weight (m_2) in an oven at 50 °C. GMF is calculated according to Eq. (1):

$$GMF(\%) = \frac{m_2}{m_1} \times 100 \quad (1)$$

Swelling behavior

Herein, a general weighing method was used to study the swelling behavior of dried hydrogels. Typically, the dry gel was soaked in deionized water at room temperature for two days, changing the water every six h to eliminate uncrosslinked components such as monomers. The gel was completely dried in a vacuum dryer. Subsequently, about 0.2 g of dry gel (m_0) was accurately weighed, and immersed in deionized water, and the mass of each swelling hydrogel was weighed periodically (m_1). The swelling degree (SR) was obtained according to Eq. (2):

$$SR(\%) = \frac{m_1 - m_0}{m_0} \times 100 \quad (2)$$

In this experiment, the pH sensitivity and thermo-sensitivity of single network hydrogels and interpenetrating network hydrogels were further studied. The pH sensitivity of single network hydrogels and interpenetrating network hydrogels was tested in the buffer solutions with pH of 2, 4, 6, 8, and 10, and the thermo-sensitivity was tested at 30 °C, 40 °C, 50 °C, and 60 °C, respectively. The buffer solutions were prepared according to Table S4. Specifically, at a fixed temperature, the hydrogel was put into different pH solutions to swell fully, and the change of its swelling degree with pH was investigated. At fixed pH, the hydrogel was fully expanded in solutions of different temperatures, and the change of swelling degree with temperature was investigated.

Deswelling behavior of hydrogels

The experimental procedure of hydrogel deswelling is as follows. About 0.2 g of dry hydrogel was accurately weighed (m_d) and soaked in deionized water at 27 °C to make it swell and reach swelling equilibrium (m_0). Subsequently, the hydrogel reached swelling equilibrium at 27 °C and was quickly immersed in deionized water at 37 °C, and the swelling mass of each sample was measured regularly (m_t). The deswelling ratio was calculated by Eq. (3).

$$WR(\%) = \frac{(m_t - m_d)}{(m_0 - m_d)} \times 100 \quad (3)$$

Drug release

The sustained release behavior of 5-Fu-loaded hydrogels in buffer solution was studied at different pH values (pH = 2.0, 8.0) and different temperatures (T = 27 °C, 37 °C). The maximum absorption wavelength of 5-Fu (λ_{Max} = 265 nm) was determined by UV-visible spectrophotometry. Typically, a conical flask, loaded with about 0.1 g of dry 5-Fu-loaded hydrogel in 50 mL buffer solution, was immersed in a constant-temperature shaker at a fixed temperature. In every preset time interval, 5 mL buffer solution was removed from the flask, and then an equal volume of fresh buffer solution was supplemented to keep the constant volume of the release medium. Each experiment was conducted three times in parallel. The cumulative 5-Fu release rate (CFR) was obtained by the following Eq. (4).

$$CFR(\%) = \frac{\sum_{i=0}^{n-1} c_i v_i + c_n V}{W} \times 100 \quad (4)$$

Where, n and i are the sampling times, C_i and C_n are respectively the concentration of 5-Fu in the solution, V_i and V are the volume of the i sampling and the total volume of the solution, respectively, and W is the weight of 5-Fu in the 5-Fu-loaded hydrogel.

Results and discussion

Poly (N, N-dimethyl acrylamide) is usually used as a hydrophilic part of hydrogel, but there are few reactive functional groups in its chain [30]. Combining maleic anhydride with

N, N-dimethyl acrylamide can make up for its deficiency. Therefore, the two monomers were selected in this experiment to prepare binary polymers by free-radical polymerization. To ensure the water solubility and reactivity of the synthetic binary polymer, the molar ratio of MAH and DMA was 1: 50 during the experiment. Gelation can occur quickly *in situ* in water by the amine-anhydride click reaction of the binary copolymer and poly(α-L-lysine), which was selected as one network of IPN hydrogel to endow hydrogel with pH sensitivity. Since the amine-anhydride reaction can proceed quickly under alkaline conditions, it is necessary to adjust the pH of the solution to alkaline with triethylamine to facilitate the ring-opening reaction of the cyclic anhydride. Additionally, PNIPAm is widely used in the preparation of intelligent hydrogels due to its temperature sensitivity, which was chosen as a main component for preparing another network of IPN hydrogels. Therefore, two single network hydrogels were combined to prepare IPN hydrogels to make the prepared hydrogels have pH and temperature sensitivity.

FT-IR analysis

FT-IR spectra of MAH, DMA, PMD, PL, CN_9, PN_{100}, and $DN_{9\text{-}100}$ are shown in Fig. 3. In the infrared spectrum of the MAH in Fig. 3A(b), the peaks at 1851 − 1777 cm^{-1} are the stretching vibration of C = O, and the peak at 1589 cm^{-1} is due to the stretching vibration of C = C. The peaks at 1244 cm^{-1} and 1052 cm^{-1} correspond to the stretching vibration of the C-O group [31]. In the infrared spectrum of DMA, the stretching vibration peak of the C-H bond presents at 2933 cm^{-1}, C = C stretching vibration peak emerges at 1652 cm^{-1}, C = O stretching vibration peak of the amide bond appears at 1604 cm^{-1} [32], C-N peak presents at 1485 cm^{-1} [33], and deformation vibration of symmetric C-H at 1402 cm^{-1} is also observed [34]. In the infrared spectrum of PMD, methyl peak appears at 2933 cm^{-1}, symmetrical methyl deformation peak is at 1402 cm^{-1}, stretching vibration peak of C-O group appears at 1052 cm^{-1}, and C = O redshift of amide bond presents at 1623 cm^{-1}. It can be seen from the infrared spectrum that the characteristic peaks of the two monomers are reflected in the binary copolymer, so it can prove that the target polymer has been successfully synthesized [35].

In the infrared spectrum of PLL (Fig. 3B(b)), the stretching vibration of N-H exhibits at 3227 cm^{-1} and 1557 cm^{-1} [36, 37], and the peak at 2878 cm^{-1} is assigned to the methylene stretching vibration. The stretching vibration of the amide bond appears at 1657 cm^{-1}, and the stretching vibration peak of C-N presents at 1248 cm^{-1} [38]. In the infrared spectrum of CN_9, the methyl stretching vibration peak appears at 2918 cm^{-1}, and the C = O stretching vibration peak is blue-shifted at 1619 cm^{-1}. The symmetrical methyl deformation vibration exhibits at 1402 cm^{-1}, and the C-N peak at 1248 cm^{-1} are observed. In the PN_{100} infrared spectrum, N-H stretching vibration peaks are located at 3282 cm^{-1}, and 1544 cm^{-1} [39], the peak at 3080 cm^{-1} is ascribed to the bending vibration of N-H, 1636 cm^{-1} is the C = O peak of the amide bond, the peak at 1462 cm^{-1} is attributed to the bending vibration of CH_2 and CH_3. C-H stretching vibration peak presents at 1181 cm^{-1} [40]. In the infrared spectrum of $DN_{9\text{-}100}$, the stretching vibration peak of the C-H appears at 2970 cm^{-1}, and the stretching vibration peak of the C = O exhibits at 1619 cm^{-1}; the symmetric methyl deformation peak at 1402 cm^{-1}, the C-N peak at 1248 cm^{-1} and the stretching vibration peak of C-O group at 1052 cm^{-1} are also observed. The above analysis indicated that the interpenetrating network hydrogel was successfully prepared.

SEM analysis

The morphology of the hydrogels was characterized by scanning electron microscope (Fig. 4). The result shows that the hydrogel samples have a relatively smooth surface, which can prevent water from entering the hydrogel quickly and slow down the release of 5-Fu. The internal morphology of the hydrogel samples is a three-dimensional porous network, which provides a large channel and interface for water

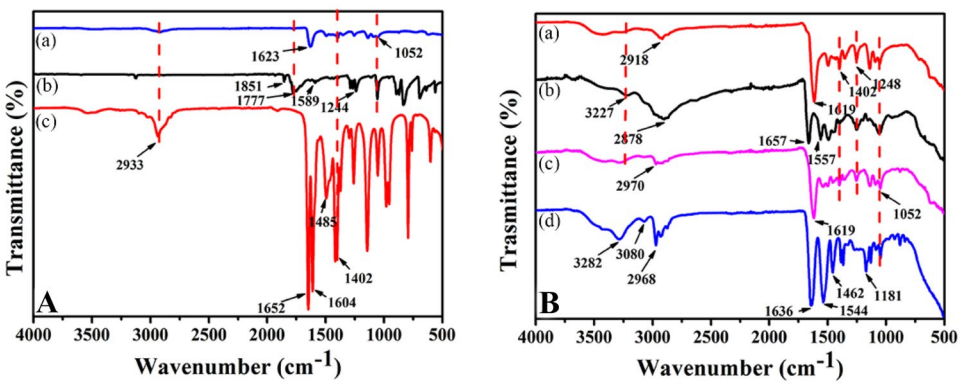

Fig. 3 FTIR spectra of the samples [**A**: PMD (**a**), MAH (**b**) and DMA (**c**); **B**: CN_9 (**a**), PLL (**b**) and $DN_{9\text{-}100}$ (**c**) and PN_{100} (**d**)]

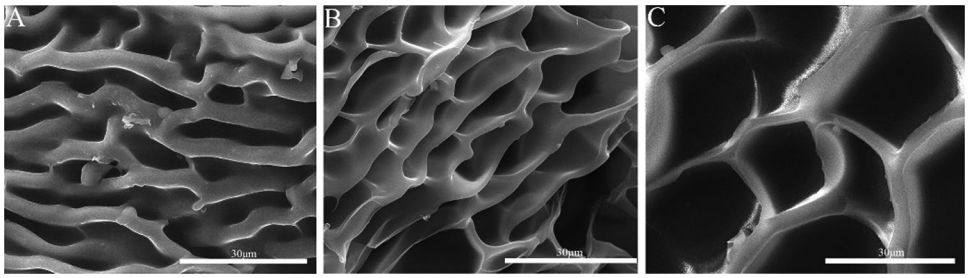

Fig. 4 SEM micrographs of CN_9 (**A**), PN_{100} (**B**), and DN_{9-100} (**C**)

molecules and drugs, so it is conducive to water absorption and drug release [41]. Compared with single network hydrogels, interpenetrating network hydrogels have interconnected three-dimensional porous structures (Fig. 4C) with a pore diameter of 27.57 micrometers (Fig. S2), which is beneficial for the application of hydrogels in the biomedical field.

XRD analysis

The aggregated structure of the hydrogel was characterized by X-ray diffraction. As shown in Fig. 5, the characteristic peaks of PN_{100} at $2\theta = 8.4°$ and 20.2° are the same as previously reported [42]. Both CN_9 and $DN_{9\text{-}100}$ have broad diffraction peaks at $2\theta = 22.4°$, indicating that the interpenetrating network structure does not cause the phase transition of the hydrogel. In addition, there is no apparent sharp diffraction peak in the figure, which indicates that the three hydrogels are mainly amorphous [43].

Optimization of raw material ratios

Gel mass fraction and swelling degree are two important parameters to measure hydrogel performance, which are affected by many factors, such as the crosslinking density of hydrogels, intermolecular forces, external pH, temperature, and ionic strength [44, 45]. Herein, gel mass fraction and swelling degree were used as two indicators to optimize the preparation conditions. Figure 6A-C depicted the influence of different raw material ratios on the gel mass fraction of hydrogels. It can be seen that the GMF of CN_n increased slightly with increasing PLL proportion. As we know, with the increase of PLL content, the number of reactive amine groups increased, leading to the increase of the collision probability and the crosslinking density of CN_n. The gel mass fraction of PN_{100} and PN_{150} has no noticeable difference. When the monomer ratio of amine group: anhydride group = 9: 1, NIPAm: MBA = 100: 1, $DN_{n\text{-}m}$ had the largest mass fraction.

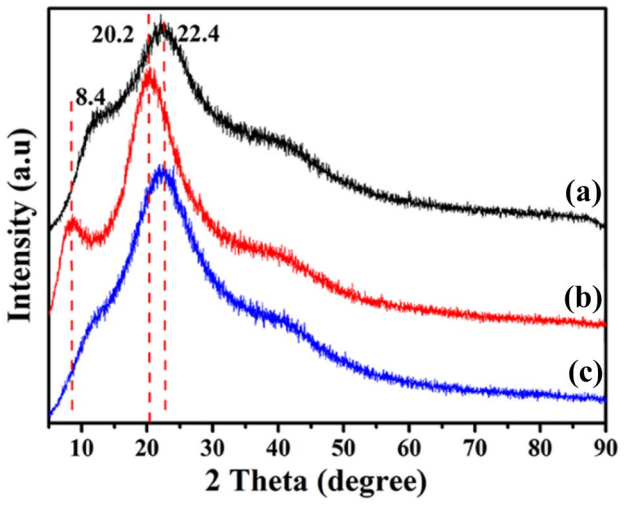

Fig. 5 XRD patterns of different samples [CN_9 (**a**), PN_{100} (**b**), $DN_{9\text{-}100}$ (**c**)]

Figure 6D-F shows the swelling behavior of hydrogels with different monomer ratios. It can be seen from Fig. 6D that the swelling degree of CN_n hydrogel increased with the increase of the molar ratio of the amine group to the anhydride group. The result can be explained as follows. When the content of poly(α-L-lysine) increased, the number of residual amine groups increased after crosslinking, resulting in the increase of the swelling degree due to that the amine groups were hydrophilic groups [46]. As described in Fig. 6E, the swelling degree of PN_n hydrogel has a decreasing tendency with the increase of MBA content. The reason is as follows. The crosslinking density of hydrogel increased when raising crosslinking agent content, resulting in the decrease of the space in the hydrogel and water absorption capacity [47]. It is clear from Fig. 6 F that when the monomer molar ratio of amine group: anhydride group = 9: 1, NIPAm: MBA = 100: 1, the swelling degree of the double network hydrogel ($DN_{9\text{-}100}$) was the largest. Compared with the single network hydrogels, the swelling degree of double network hydrogels was basically between that of the two single networks, which further confirmed that the swelling behavior of interpenetrating network hydrogels was the result of the interaction of two single networks. Considering $DN_{9\text{-}100}$ IPN hydrogel had the largest swelling degree and gel mass fraction, $DN_{9\text{-}100}$ IPN hydrogel and corresponding CN_9 hydrogel and PN_{100} hydrogel were used for subsequent experiments and characterization.

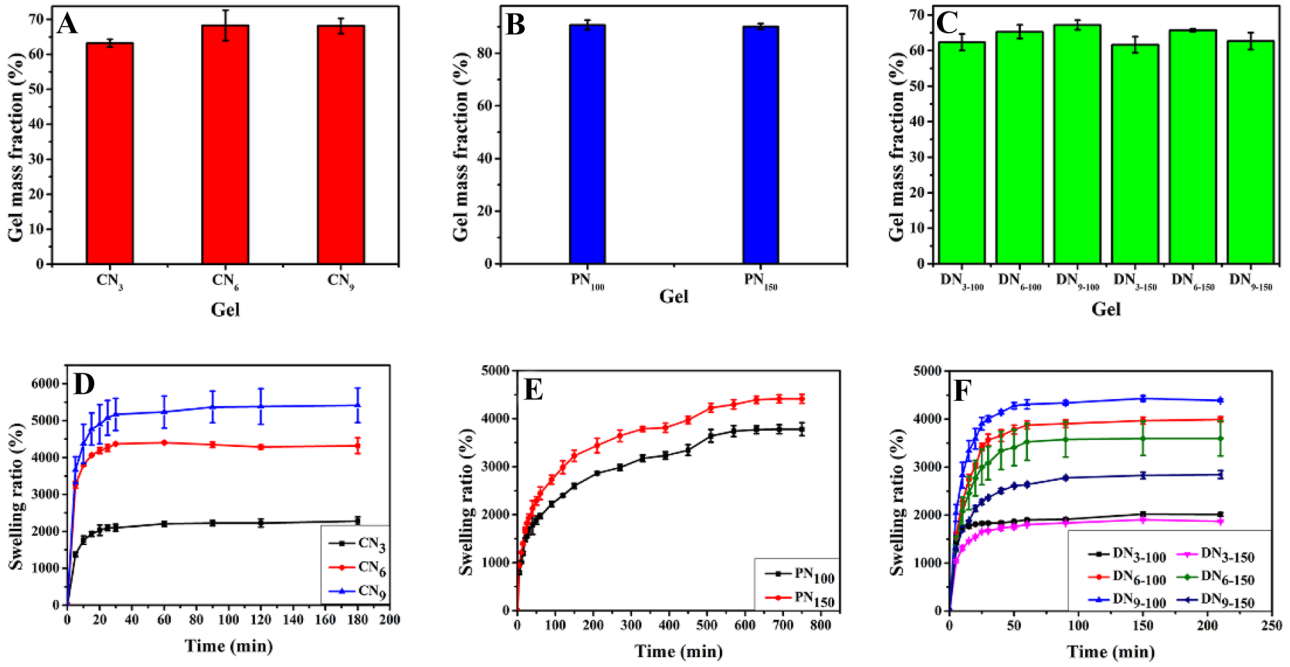

Fig. 6 Gel mass fractions and swelling curves of CN_n (**A**, **D**), PN_n (**B**, **E**), and $DN_{n\text{-}m}$ (**C**, **F**) at 30 °C and pH = 7

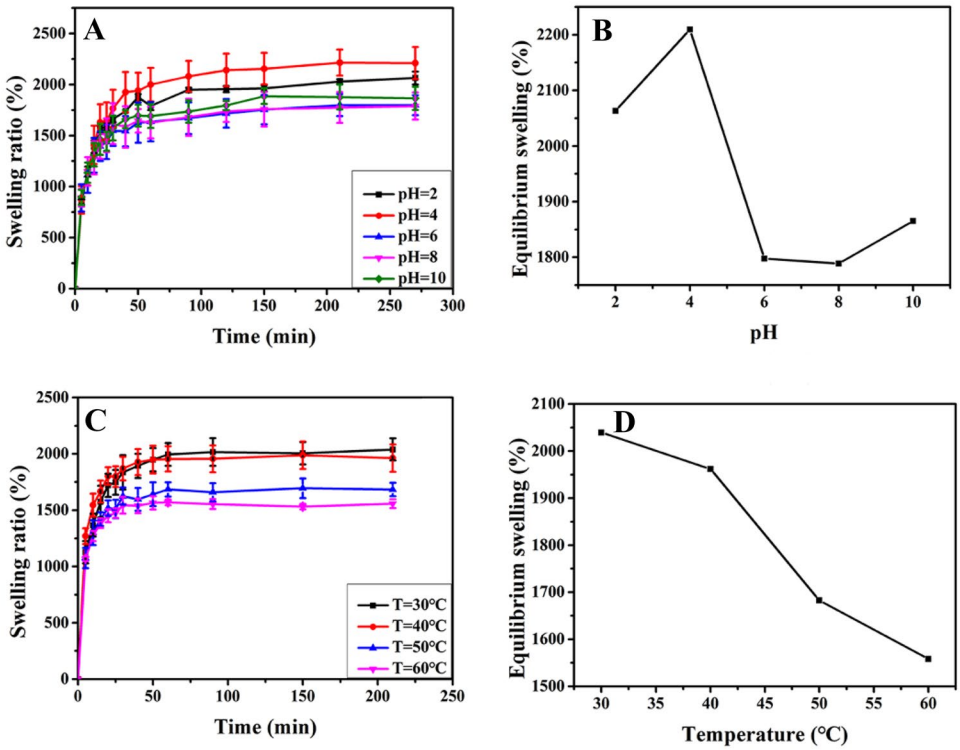

Fig. 7 Swelling ratios (**A**, **C**) and equilibrium swelling ratios (**B**, **D**) of $DN_{9\text{-}100}$ under different pH values (30 °C) and temperatures (pH = 4)

Swelling behavior of IPN-Gel $DN_{9\text{-}100}$ at different pH and temperature

Figure 7A, B show the swelling behavior of DN_{9-100} hydrogel at different pH. When pH changed from 2 to 4, its equilibrium swelling ratio increased; when pH increased from 4 to 6, the equilibrium swelling ratio decreased sharply. However, when pH varied from 6 to 10, the equilibrium swelling ratio had a growing tendency. pH sensitivity of the hydrogel mainly resulted from the network formed by poly(α-L-lysine) and the binary copolymer, due to the existence of NH_2 and COOH. When the solution pH was low, most of the amine groups in the hydrogel were positively charged and became the form of NH_3^+. The electrostatic repulsion between NH_3^+ could lead to the polymer network swelling and a large amount of water entering the hydrogel network [48]. When the pH value increased, the NH_3^+ gradually deprotonated into NH_2, and the carboxyl group existed mainly in the form of COOH. At this time, intermolecular and intramolecular hydrogen bonds in the hydrogel became the main interaction of the polymer network, resulting in the increase of the hydrophobicity of the network and the decrease of the swelling degree. However, when pH continued to increase, the carboxylic acid deprotonated into $-COO^-$, and the electrostatic repulsion between $-COO^-$ predominated, which would result in the increase in the swelling degree of hydrogel [49]. Of course, the ion concentration of the buffer solution would also influence the swelling ratio of the hydrogel.

Figure 7C, D show that the swelling degree of DN_{9-100} hydrogel decreased with the increase of the temperature, which was the comprehensive result of the interaction between hydrophilic and hydrophobic groups. As we know, there are hydrophilic amide groups and hydrophobic isopropyl groups on PNIPAm chains. The amide groups could interact with water molecules to form hydrogen bonds when the temperature was low, inducing more water absorbed into the hydrogel and higher swelling degree. At higher temperatures, hydrophobic interactions between isopropyl groups and water dominated, few hydrogen bonds were formed, so the swelling degree was low [50].

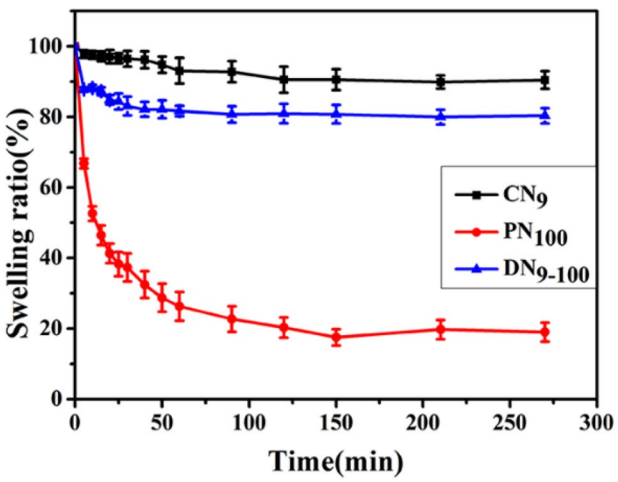

Fig. 9 Deswelling kinetics of hydrogels in deionized water when the temperature

Figure 8A, B show reversibility and repeatability of the swelling behavior of double-network hydrogels at different pH and temperature. Obviously, the pH sensitivity and temperature sensitivity of the hydrogel are reversible and repeatable, which is of importance to the application of smart hydrogels.

Deswelling behavior of hydrogels

As shown in Fig. 9, the swelling degree of CN_9 hydrogel in deionized water decreased slightly from 27 °C to 37 °C. It indicates that the hydrogel had an insignificant temperature response when the temperature changed. However, PN_{100} hydrogel and DN_{9-100} hydrogel had a higher water loss rate when the temperature changed, especially in the first 20 min. It indicates that these two hydrogels had better temperature sensitivity. With the extension of time, the water loss rate of hydrogel increased and finally reached a stable state. The water loss rate of the double network hydrogel was less than that of the single network hydrogel PN_{100}, which indicates that the temperature sensitivity decreased after forming the interpenetrating network hydrogel.

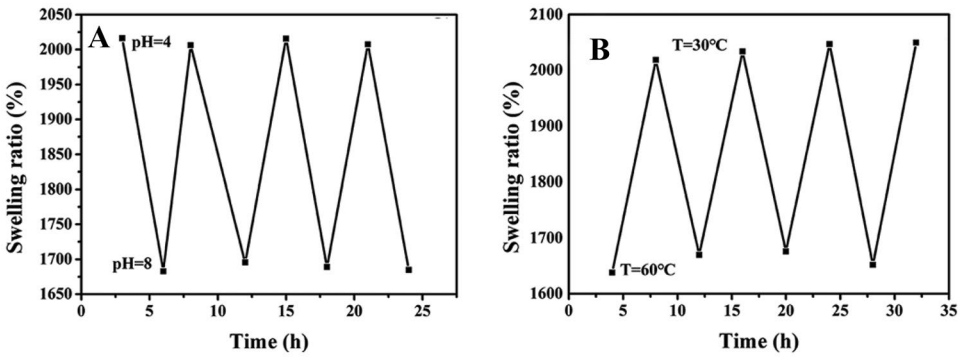

Fig. 8 Swelling cycles of DN_{9-100} IPN-Gel under different pH values (30 °C) (**A**) and different temperatures (pH = 4) (**B**)

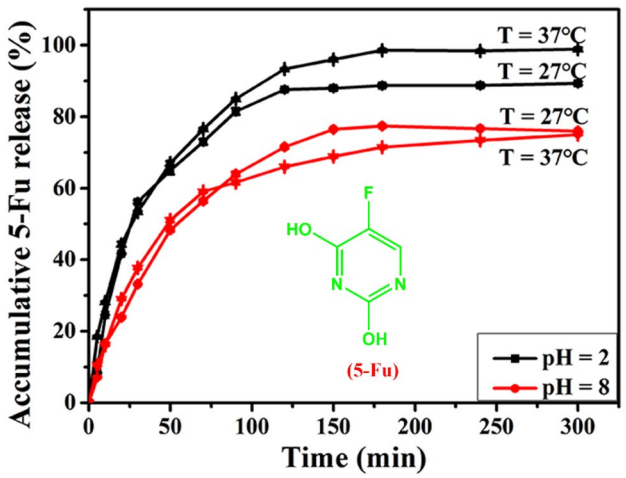

Fig. 10 Release curves of 5-Fu in DN_{9-100} IPN-Gel; the inset image shows the structure of 5-Fu

changed from 27 °C to 37 °C.

In vitro 5-Fu sustained-release analysis

5-Fu, containing acidic phenolic hydroxyl and alkaline amino groups (Fig. 10) [51], was chosen as a sustained-release model drug, the drug release performance of double-network hydrogels $DN_{9\text{-}100}$ at different pH and temperature in vitro was studied. In general, drug release performance is deeply influenced by the swelling behavior of carriers, drug solubility as well as interactions between drug and carriers [52]. As known in Fig. 10, the release of 5-Fu showed an explosive release in the initial stage, followed by a slowing trend of release rate [53]. The possible reason is that some drug was on the surface of the hydrogel and not tightly bound by the polymer chain. When the temperature remained constant, the accumulative release of 5-Fu at pH = 2 was greater than that at pH = 8, indicating an acidic medium was conducive to release, which was due to the more swelling of the hydrogel at pH = 2 (Fig. 7B) [52]. Additionally, the remaining amino groups on the PLL could be protonated under acidic conditions, producing electrostatic repulsive interaction with protonated 5-Fu, which accelerated the release of 5-Fu [54]. Instead, when pH = 8, the amino groups were deprotonated, forming a hydrogen bond between the fluorine group of 5-Fu and the amino groups of PLL, which delayed the release of 5-Fu [55]. When pH = 2, the accumulative release of 5-Fu at 37 °C was greater than that at 27 °C, while pH = 8, the accumulative release of 5-Fu at 37 °C was slightly lower than that at 27 °C. The results indicate the release behavior of 5-Fu in the hydrogel can be adjusted by controlling temperature and pH.

Kinetic analysis of drug release in vitro

To investigate the 5-Fu drug release mechanism from the hydrogel, zero-order (Table S5), first-order (Table S6), Higuchi (Table S7), and Korsmeyer-Peppas kinetic models (Table S8) were used to simulate the experimental data [56]. The Korsmeyer-Peppas kinetic model (Eq. 5) was more suitable to simulate the release process of the IPN hydrogel $DN_{9\text{-}100}$.

$$\frac{M_t}{M_\infty} = kt^n \tag{5}$$

Where M_t is the drug release amount at time t, M_∞ is the drug release amount at equilibrium, k is the characteristic constant of hydrogel, and n is the diffusion index. The model is valid for M_t/M_∞ less than 0.6 [57]. When the drug-loaded polymer matrix is immersed in the medium, the drug is released in three steps. First, the water in the system enters the matrix, resulting in the swelling of the hydrogel. In the second step, the polymer relaxes. In the third step, the drug diffuses from the matrix into the surrounding medium. The release mechanism of drug diffusion from the polymer matrix to the medium can be divided into Fickian diffusion, non-Fickian diffusion, and Case II diffusion [58]. In the case of a cylinder, when $n \leq 0.45$, it indicates Fickian diffusion, so the relaxation rate is greater than the diffusion rate; When $0.45 < n < 0.89$, it indicates the non-Fickian diffusion, and the relaxation rate and diffusion are comparable; When $n > 0.89$, it suggests that the case II diffusion takes place, and the diffusion rate is faster than the relaxation rate; When $n > 1$, drug release follows the super case II diffusion [59]. The values of n were calculated from the slope of $log\left(\frac{M_t}{M_\infty}\right)$ and $logk$ under acidic and alkaline conditions according to Eq. (6) [60].

$$log\left(\frac{M_t}{M_\infty}\right) = logk + nlogt \tag{6}$$

As shown in Table S8, when pH = 8, the n values were greater than 0.45 and less than 0.89 whether at 27 °C or 37 °C, indicating non-Fickian diffusion. When pH = 2, the n value was greater than 0.45 and less than 0.89 at 37 °C, suggesting non-Fickian diffusion; while at 27 °C, the n value was greater than0.89, implying the case II diffusion.

Conclusions

In summary, poly(α-L-lysine) -based interpenetrating network hydrogels with pH sensitivity and thermo-sensitivity could be prepared by synchronous amine-anhydride click reaction and free radical polymerization in water. The swelling behavior and drug release behavior were studied. The results show that the prepared IPN hydrogels are pH and temperature sensitive, and the pH and temperature responsiveness are closely related to the

stimulus responsiveness of the corresponding single-network hydrogels. The controlled release behavior of prepared IPN hydrogels is closely related to its swelling behavior, and the drug release rate can be adjusted by controlling pH and temperature. The drug release behavior can be described by korsmeyer-Peppas model. The strategy described here for preparing interpenetrating network hydrogel is simple, and the reaction conditions are mild, which has a wide application prospect in hydrogel preparation.

Supplementary information The online version contains supplementary material available at https://doi.org/10.1007/s10965-022-03054-x.

Acknowledgements The work was supported by Natural Science Project of Zhengzhou Science and Technology Bureau [grant number 21ZZXTCX14]; the Innovative Funds Plan of Henan University of Technology [grant number: 2021ZKCJ08]; Henan University of Technology [grant number: HAUTZX202003]; the National Natural Science Foundation of China [grant number: U1904171]; the Key Science and Technology Project of Henan Province, China [grant number: 212102210630].

Declarations

Conflict of interest The authors declare that they have no known competing financial interests or personal relationships that could have appeared to influence the work reported in this paper.

References

1. Hoffman AS (2012) Hydrogels for biomedical applications. Adv Drug Delive Rev 64:18–23
2. Phan VHG, Thambi T, Gil MS, Lee DS (2017) Temperature and pH-sensitive injectable hydrogels based on poly(sulfamethazine carbonate urethane) for sustained delivery of cationic proteins. Polymer 109:38–48
3. Chen Z, Liu J, Chen Y, Zheng X, Liu H, Li H (2021) Multiple-stimuli-responsive and cellulose conductive ionic hydrogel for smart wearable devices and thermal actuators. ACS Appl Mater Inter 13(1):1353–1366
4. Yu HT, Guo YT, Yao C, Perepichka DF, Meng H (2016) A smart polymer with a high sensitivity to temperature and humidity based on polyacrylamide hydrogel doped with polyiodide. J Mater Chem C 4(47):11055–11058
5. Shi Q, Liu H, Tang DD, Li YH, Li XJ, Xu F (2019) Bioactuators based on stimulus-responsive hydrogels and their emerging biomedical applications. NPG Asia Mater 11:64
6. Zhan JH, Wu YJ, Wang HH, Liu JL, Ma QZ, Xiao KC, Li Z, Li J, Luo F, Tan H (2020) An injectable hydrogel with pH-sensitive and self-healing properties based on 4armPEGDA and N-carboxyethyl chitosan for local treatment of hepatocellular carcinoma. Int J Biol Macromol 163:1208–1222
7. Scarpa E, Mastronardi VM, Guido F, Algieri L, Qualtieri A, Fiammengo R, Rizzi F, De Vittorio M (2020) Wearable piezoelectric mass sensor based on pH sensitive hydrogels for sweat pH monitoring. Sci Rep 10(1):10854
8. Gau E, Flecken F, Ksiazkiewicz AN, Pich A (2018) Enzymatic synthesis of temperature-responsive poly(N-vinylcaprolactam) microgels with glucose oxidase. Green Chem 20(2):431–439
9. Grishkewich N, Akhlaghi SP, Yao ZL, Berry R, Tam KC (2016) Cellulose nanocrystal-poly(oligo(ethylene glycol) methacrylate) brushes with tunable LCSTs. Carbohydr Polym 144:215–222
10. Liao J, Huang HH (2019) Temperature/pH dual sensitive Hericium erinaceus residue carboxymethyl chitin/poly (N-isopropyl acrylamide) sequential IPN hydrogels. Cellulose 27(2):825–838
11. Liu Y, Zhang KH, Ma JH, Vancso GJ (2017) Thermoresponsive semi-IPN hydrogel microfibers from continuous fluidic processing with high elasticity and fast actuation. ACS Appl Mater Inter 9(1):901–908
12. Raghuwanshi VS, Garnier G (2019) Characterisation of hydrogels: Linking the nano to the microscale. Adv Colloid Interface Sci 274(2):102044
13. Rezvanian M, Ahmad N, Amin MCIM, Ng SF (2017) Optimization, characterization, and in vitro assessment of alginate-pectin ionic cross-linked hydrogel film for wound dressing applications. Int J Biol Macromol 97:131–140
14. Nezhad-Mokhtari P, Ghorbani M, Roshangar L, Rad JS (2019) A review on the construction of hydrogel scaffolds by various chemically techniques for tissue engineering. Eur Polym J 117:64–76
15. Kloxin CJ, Bowman CN (2013) Covalent adaptable networks: smart, reconfigurable and responsive network systems. Chem Soc Rev 42(17):7161–7173
16. Arkenberg MR, Nguyen HD, Lin CC (2020) Recent advances in bio-orthogonal and dynamic crosslinking of biomimetic hydrogels. J Mater Chem B 8(35):7835–7855
17. Li JH, Wu CT, Chu PK, Gelinsky M (2020) 3D printing of hydrogels: Rational design strategies and emerging biomedical applications. Mater Sci Eng R Rep 140:100543
18. Zhao JW, Narita T, Creton C (2020) Dual crosslink hydrogels with metal-ligand coordination bonds: Tunable dynamics and mechanics under large deformation. Adv Polym Sci 285:1–20
19. Bao ZT, Xian CH, Yuan QJ, Liu GT, Wu J (2019) Natural polymer-based hydrogels with enhanced mechanical performances: Preparation, structure, and property. Adv Healthc Mater 8(17):e1900670
20. Noh W, Kim J, Lee SJ, Ryu BG, Kang CM (2018) Harvesting and contamination control of microalgae Chlorella ellipsoidea using the bio-polymeric flocculant alpha-poly-l-lysine. Bioresour Technol 249:206–211
21. Zheng M, Pan M, Zhang W, Lin H, Wu S, Lu C, Tang S, Liu D, Cai J (2021) Poly(alpha-l-lysine)-based nanomaterials for versatile biomedical applications: Current advances and perspectives. Bioact Mater 6:1878–1909
22. Kokufuta MK, Sato S, Kokufuta E (2011) Swelling-shrinking behavior of chemically cross-linked polypeptide gels from poly(alpha-L-lysine), poly(alpha-DL-lysine), poly(varepsilon-L-lysine) and thermally prepared poly(lysine): effects of pH, temperature and additives in the solution. Colloids Surf B Biointerfaces 87:299–309
23. Guo JH, Wei CZ, Wang XT, Hou YT, Guo WH (2021) An in situ mechanical adjustable double crosslinking hyaluronic acid/polylysine hydrogel matrix: Fabrication, characterization and cell morphology. Int J Biol Macromol 180:234–241
24. Divakaran AV, Azad LB, Surwase SS, Torris ATA, Badiger MV (2016) Water-stable plasma-polymerized N, N-dimethylacrylamide coatings to control cellular adhesion. Chem Mater 28(7):2120–2130
25. Dhand AP, Galarraga JH, Burdick JA (2020) Enhancing biopolymer hydrogel functionality through interpenetrating networks. Trends Biotechnol 39(5):519–538
26. Yuk H, Lu BY, Zhao XH (2019) Hydrogel bioelectronics. Chem Soc Rev 48(6):1642–1667
27. Saruchi KV, Mittal H, Alhassan SM (2019) Biodegradable hydrogels of tragacanth gum polysaccharide to improve water retention capacity of soil and environment-friendly controlled release of agrochemicals. Int J Biol Macromol 132:1252–1261

28. Wang J, Liu C, Shuai Y, Cui X, Nie L (2014) Controlled release of anticancer drug using graphene oxide as a drug-binding effector in konjac glucomannan/sodium alginate hydrogels. Colloids Surf B Biointerfaces 113:223–229
29. Zhu L, Ma J, Jia N, Zhao Y, Shen H (2009) Chitosan-coated magnetic nanoparticles as carriers of 5-fluorouracil: preparation, characterization and cytotoxicity studies. Colloids Surf B Biointerfaces 68:1–6
30. Afroz S, Afrose F, Alam AKMM, Khan RA, Alam MA (2018) Synthesis and characterization of polyethylene oxide (PEO)—N,N-dimethylacrylamide (DMA) hydrogel by gamma radiation. Adv Compos Hybrid Mater 2(1):133–141
31. Dinari M, Atabaki F, Pahnavar Z, Soltani R (2020) Adsorptive removal properties of bivalent cadmium from aqueous solution using porous poly(N-2-methyl-4-nitrophenyl maleimide-maleic anhydride-methyl methacrylate) terpolymers. J Environ Chem Eng 8(6):104560
32. Wu ZJ, Zhang JJ, Lin QQ, Zhu YL, Wang L, Li YJ (2021) Movable-crosslinking tough hydrogels with lithium ion as sensitive and durable compressive sensor. Polymer 214:123257
33. Bashir S, Omar FS, Hina M, Numan A, Iqbal J, Ramesh S, Ramesh K (2020) Synthesis and characterization of hybrid poly (N, N-dimethylacrylamide) composite hydrogel electrolytes and their performance in supercapacitor. Electrochim Acta 332:135438
34. Egghe T, Cools P, Van Guyse JFR, Asadian M, Khalenkow D, Nikiforov A, Declercq H, Skirtach AG, Morent R, Hoogenboom R, De Geyter N (2020) Water-stable plasma-polymerized N, N-dimethylacrylamide coatings to control cellular adhesion. ACS Appl Mater Inter 12(2):2116–2128
35. Sheikhy S, Safekordi AA, Ghorbani M, Adibkia K, Hamishehkar H (2021) Synthesis of novel superdisintegrants for pharmaceutical tableting based on functionalized nanocellulose hydrogels. Int J Biol Macromol 167:667–675
36. Dutta S, Chowdhury T, Ghosh AK (2020) Green synthesis of poly-L-lysine-coated sericin nanoparticles and their molecular size-dependent antibacterial activity. Colloids Surf B Biointerfaces 188:110822
37. Shen JM, Chen J, Ma JB, Fan LL, Zhang XL, Yue T, Yan YP, Zhang YH (2020) Enhanced lysosome escape mediated by 1,2-dicarboxylic-cyclohexene anhydride-modified poly-l-lysine dendrimer as a gene delivery system. Asian j Pharm sci 15(6):759–776
38. Liu JN, Chang SL, Xu PW, Tan MH, Zhao B, Wang XD, Zhao QS (2020) Structural changes and antibacterial activity of epsilon-poly-l-lysine in response to pH and phase transition and their mechanisms. J Agric Food Chem 68(4):1101–1109
39. Shin Y, Choi J, Na JH, Kim SY (2021) Thermally triggered soft actuators based on a bilayer hydrogel synthesized by gamma ray irradiation. Polymer 212:123163
40. Eftekhari-Sis B, Rahimkhoei V, Akbari A, Araghi HY (2018) Cubic polyhedral oligomeric silsesquioxane nano-cross-linked hybrid hydrogels: Synthesis, characterization, swelling and dye adsorption properties. React Funct Polym 128:47–57
41. Wei HL, Geng LF, Zhu HZ, Li JJ (2019) Facile fabrication of thermosensitive hydrogel microspheres based on a combination of metal-free click chemistry and spray drying. Chem Eng Process 136:116–122
42. Ribeiro CA, Martins MVS, Bressiani AH, Bressiani JC, Leyva ME, de Queiroz AAA (2017) Electrochemical preparation and characterization of PNIPAM-HAp scaffolds for bone tissue engineering. Mat Sci Eng C- Mater 81:156–166
43. Wei HL, Yang XQ, Chu HJ, Li JJ (2019) Facile and green preparation of thermal and pH sensitive hydrogel microspheres based on spray drying and the diels–alder reaction. Polym Eng Sci 59(10):1999–2007
44. Boral S, Gupta AN, Bohidar HB (2006) Swelling and de-swelling kinetics of gelatin hydrogels in ethanol-water marginal solvent. Int J Biol Macromol 39(4–5):240–249
45. Hamedi S, Shojaosadati SA, Najafi V, Alizadeh V (2020) A novel double-network antibacterial hydrogel based on aminated bacterial cellulose and schizophyllan. Carbohydr Polym 229:115383
46. Oh J, Jung KI, Jung HW, Khan A (2019) A modular and practical synthesis of zwitterionic hydrogels through sequential amine-epoxy "click" chemistry and n-alkylation reaction. Polymers 11(9):1491
47. Song WJ, Xin JN, Zhang JW (2017) One-pot synthesis of soy protein (SP)-poly(acrylic acid) (PAA) superabsorbent hydrogels via facile preparation of SP macromonomer. Ind Crops Prod 100:117–125
48. Brahim S, Narinesingh D, Guiseppi EA (2003) Synthesis and hydration properties of pH-sensitive p(HEMA)-based hydrogels containing 3-(trimethoxysilyl)propyl methacrylate. Biomacromolecules 4(3):497–503
49. Xu K, Tan Y, Chen Q, An HY, Li WB, Dong LS, Wang PX (2010) A novel multi-responsive polyampholyte composite hydrogel with excellent mechanical strength and rapid shrinking rate. J Colloid Interface Sci 345(2):360–368
50. Hebeish A, Farag S, Sharaf S, Shaheen TI (2014) Thermal responsive hydrogels based on semi interpenetrating network of poly(NIPAm) and cellulose nanowhiskers. Carbohydr Polym 102:159–166
51. Han J, Wang K, Yang D, Nie J (2009) Photopolymerization of methacrylated chitosan/PNIPAAm hybrid dual-sensitive hydrogels as carrier for drug delivery. Int J Biol Macromol 44:229–235
52. El-Sherbiny IM, Smyth HD (2010) Poly(ethylene glycol)-carboxymethyl chitosan-based pH-responsive hydrogels: photo-induced synthesis, characterization, swelling, and in vitro evaluation as potential drug carriers. Carbohydr Res 345:2004–2012
53. Chang GR, Chen Y, Li YJ, Li SK, Huang FZ, Shen YH, Xie AJ (2015) Self-healable hydrogel on tumor cell as drug delivery system for localized and effective therapy. Carbohydr Polym 122:336–342
54. Jin H, Liu X, Gui R, Wang Z (2015) Facile synthesis of gold nanorods/hydrogels core/shell nanospheres for pH and near-infrared-light induced release of 5-fluorouracil and chemo-photothermal therapy. Colloids Surf B Biointerfaces 128:498–505
55. Pancholi NJ, Sonker N, Bajpai J, Bajpai AK (2020) Predictions of drug-protein Interactions and study of Magnetically Assisted Release dynamics of 5-fluorouracil from soya protein-coated Iron oxide rore-Shell Nanoparticles. ACS Appl Bio Mater 3:3170–3186
56. Rao KM, Nagappan S, Seo DJ, Ha CS (2014) pH sensitive halloysite-sodium hyaluronate/poly(hydroxyethyl methacrylate) nanocomposites for colon cancer drug delivery. Appl Clay Sci 97–98:33–42
57. Costa P, Lobo JMS (2001) Modeling and comparison of dissolution profiles. Eur J Pharm Sci 13:123–133
58. Dey KP, Mishra S, Chandra N (2017) Colon targeted drug release studies of 5-ASA using a novel pH sensitive polyacrylic acid grafted barley. Polym Bull 74(8):3431–3453
59. Siepmann J, Peppas NA (2011) Higuchi equation: derivation, applications, use and misuse. Int J Pharm 418:6–12
60. Bardajee GR, Hooshyar Z, Asli MJ, Shahidi FE, Dianatnejad N (2014) Synthesis of a novel supermagnetic iron oxide nanocomposite hydrogel based on graft copolymerization of poly((2-dimethylamino)ethyl methacrylate) onto salep for controlled release of drug. Mat Sci Eng C- Mater 36:277–286